

Thermodynamic and Structural Properties of Ball-milled Mixtures Composed of Nano-Structural Graphite and Alkali(-Earth) Metal Hydride

Hiroki Miyaoka, ^aTakayuki Ichikawa* and ^aHironobu Fujii

*Department of Quantum Matter, ADSM, Hiroshima University, 1-3-1 Kagamiyama,
Higashi-Hiroshima 739-8530, Japan.*

^a*Institute for Advanced Materials Research, Hiroshima University, 1-3-1 Kagamiyama,
Higashi-Hiroshima 739-8530, Japan.*

Abstract

Hydrogen desorption properties of mechanically milled materials composed of nano-structural hydrogenated-graphite ($C^{\text{nano}}H_x$) and alkali(-earth) metal hydride (MH; M = Na, Mg and Ca) were investigated from the thermodynamic and structural points of view. The hydrogen desorption temperature for all the $C^{\text{nano}}H_x$ and MH composites was obviously lower than that of the corresponding each hydride. In addition, the desorption of hydrocarbons from $C^{\text{nano}}H_x$ was significantly suppressed by making composite of $C^{\text{nano}}H_x$ with MH, even though $C^{\text{nano}}H_x$ itself thermally desorbs a considerably large amount of hydrocarbons. These results indicate that an interaction exists between $C^{\text{nano}}H_x$ and MH, and hydrogen in both the phases is destabilized by a close contact between polar C-H groups in $C^{\text{nano}}H_x$ and the MH solid phase. Moreover, a new type of chemical bonding between the nano-structural carbon (C^{nano}) and the Li, Ca, or Mg metal atoms may be formed after hydrogen desorption. Thus, the above metal-C-H system would be recognized as a new family of H-storage materials.

*Corresponding author: T. Ichikawa, E-mail: tichi@hiroshima-u.ac.jp, Phone & Fax: +81-82-424-5744

Keywords: (A) hydrogen absorbing materials, nanostructured materials, (B) solid state reactions, (C) thermodynamic properties, (D) thermal analysis

1. INTRODUCTION

At present, the research and development of high-performance hydrogen storage (H-storage) materials have been continued to establish the suitable H-storage and transportation technologies as practical uses for creating a clean and sustainable energy system. In particular, hydrogen storage materials composed of light elements such as lithium (Li), carbon (C), boron (B), nitrogen (N) and sodium (Na) have been paid attention as on-board applications because of expecting to have a large mass as well as volumetric density effectively. Since Dillon *et al.* reported on hydrogen adsorption properties in single wall carbon nano-tubes [1-7], some new carbon materials such as carbon nano-fiber [8-10], activated carbon [11, 12] and hydrogenated nano-structural graphite ($C^{\text{nano}}H_x$) [13-18] have been investigated as promising H-storage materials all over the world because those are outstanding in an abundant resource and the economical and safety advantages.

Among them, we have paid attention to the $C^{\text{nano}}H_x$ product prepared by ballmilling graphite under a H_2 -gas atmosphere as one of the future energy storage systems. The nano-structural feature and the hydrogenation in the product are simultaneously induced during mechanically milling process under the H_2 -gas atmosphere. So far, it has been found that a large amount of hydrogen (~7 mass%) is chemisorbed in the $C^{\text{nano}}H_x$ product with the form of -CH, -CH₂ or -CH₃ groups at the graphene edges during

ballmilling [19, 20]. With respect to the thermal desorption properties, not only hydrogen H_2 but also hydrocarbons CH_4 and C_2H_6 were desorbed from the $C^{nano}H_x$ product in the temperature range from 300 to 800 °C, which corresponds to more than 30 mass% weight loss [21]. However, their desorption temperatures were recognized to be too high for the practical use. Moreover, it has been found that a graphitization in the product also proceeds above 700 °C [17]. The above results indicate that the $C^{nano}H_x$ product itself is useless for hydrogen storage materials, and some further breakthroughs are needed to improve the hydrogen storage properties of the $C^{nano}H_x$ product for practical uses.

On the basis of the above background, we have recently paid attention to the following chemical reaction;



which is one of the elementary reactions in the Li-N-H system [22]. This reaction proceeds even at room temperature and the system releases hydrogen. This indicates that the stable ionic crystal LiH is destabilized by reacting with a polar molecule NH_3 . On the analogy of this reaction, we have designed a novel hydrogen storage system using a reaction between $C^{nano}H_x$ and LiH, where the hydrocarbons group is polarized in the $C^{nano}H_x$ product just like ammonia molecule as is clear from the existence of the IR active modes corresponding to the C-H bonding [19], so that it is considered that $C^{nano}H_x$ should easily react with LiH.

The composite of $C^{nano}H_x$ and LiH, which is called as the Li-C-H system, were synthesized by mechanically ball-milling the mixture of $C^{nano}H_x$ and LiH powder to get a close contact with each other. The result of thermal gas-desorption measurement revealed that the hydrogen desorption temperature of the composite was much lower

than that of each component. In addition, a quite small amount of hydrocarbons were simultaneously desorbed with the hydrogen desorption as well, even though a considerably large amount of hydrocarbons were released from $C^{\text{nano}}H_x$ itself without making composite with LiH. This behavior indicates that hydrogen in $C^{\text{nano}}H_x$ and LiH could be destabilized by an interaction between the polarized parts and the ionic solid [21] and is released at lower temperature than that from the host products themselves. Furthermore, no evident peak was observed in the XRD pattern for the composite after dehydrogenation, indicating that nano-structural phase induced by mechanical milling persists to be a thermodynamically stable phase even after hydrogen desorption. Due to such thermodynamic and structural properties, the composite reversibly absorbs/desorbs about 4.5 mass% of hydrogen below 350 °C [23]. However, hydrogen absorption/desorption mechanism and the state of hydrogen atoms absorbed in the composite have not been clarified yet. It is important to understand hydrogen storage mechanism in metal-C-H systems from the fundamental and applicable points of view for developing metal-C-H systems as hydrogen storage materials for on-board applications.

In this paper, we report the hydrogen storage properties of ball-milled materials composed of the $C^{\text{nano}}H_x$ product and alkaline(-earth) metal hydride (MH ; M = Na, Mg and Ca). This work is systematically undertaken to understand the hydrogen storage mechanism of metal-C-H materials. From their thermodynamic and structural properties, we approach the issue why hydrogen in the metal-C-H composites is released at lower temperature than those of the constituent products themselves.

2. EXPERIMENTAL

The $C^{\text{nano}}H_x$ product was prepared by ballmilling high purity graphite powder (99.999 %, STREAM CHEMICALS) using a rocking (vibrating) ballmill equipment (SEIWA GIKEN Co. Ltd., RM-10). Then, 300 mg graphite powder and 20 ZrO_2 balls with 8 mm in diameter were put into a milling vessel with an inner volume of $\sim 30 \text{ cm}^3$ made of Cr steel (SKD-2) and the graphite was milled for 80 h under a 1 MPa H_2 at room temperature. After that, the mixtures of the $C^{\text{nano}}H_x$ product and MH (M =Na, Mg and Ca) were mechanically milled for 2 h under the 1 MPa H_2 -gas atmosphere by using a planetary (rotating) ballmill equipment (Fritch, P7), in which totally 300 mg of the $C^{\text{nano}}H_x$ product and MH mixture and 20 ZrO_2 balls put into the Cr steel vessel. As references, mechanically milled powders of NaH and CaH_2 were also prepared as well. Here, the purities of NaH, MgH_2 and CaH_2 used in this work were 95 % (Aldrich), 95 % (GELEST INC.) and 99.99 % (Aldrich), respectively. The molar ratio of $C^{\text{nano}}H_x$ and MH was chosen to be the ratio of C (in the $C^{\text{nano}}H_x$)/H (in the MH) ~ 2 .

All the samples were handled in a glovebox (Miwa MFG, MP-P60W) filled with a purified argon (> 99.9999 %) to avoid an oxidation and a pollution due to water. Thermal gas-desorption properties and thermodynamic properties of as-prepared composites were examined by a thermal desorption mass spectroscopy (TDMS) (Anelva, M-QA200TS) equipment connected with thermogravimetry (TG) and differential scanning calorimetry (DSC) (Q10 PDSC, TA Instruments). Especially, these equipments are installed inside the glovebox so as to minimize an influence of exposing the samples to air. In the TG-TDMS and DSC measurements, a highly purified helium gas (> 99.9999 %) and a high quality argon gas (> 99.999 %) were used as carrier gases, respectively. Here, a heating rate was fixed to be $5 \text{ }^\circ\text{C}/\text{min}$ for all the composites studied in this work. Structural properties of the composites were examined by the X-ray

diffraction measurement (XRD) (Rigaku, RINT-2100, CuK α radiation), where all the samples were specially covered by a polyimide sheet (Kapton[®], Du Pont-Toray Co., LTD.) in the glovebox to minimize an oxidation.

3. RESULTS AND DISCUSSION

3.1 Hydrogen storage properties of the C^{nano}H_x+NaH composite

As shown in inset of Figure 1(a), the TDMS profile indicates that the milled NaH needs 320 °C to release hydrogen gas under a purified helium flow. However, the C^{nano}H_x and NaH composite exhibits a broad sub-peak at slightly lower temperature than the temperature corresponding to a main peak for hydrogen desorption, where these peaks are located around 260 and 300 °C, respectively. It should be noted that their hydrogen desorption temperatures are lower than those of constituent components. Accompanied by the lower hydrogen desorption corresponding to 260 °C, it is noticed that quite small amount of hydrocarbons are desorbed from the composite as well. However, the hydrocarbons desorption is immediately suppressed with further increasing temperature after showing a broad peak around 260 °C, indicating that the hydrogen gas is desorbed instead of hydrocarbons due to an interaction between the C^{nano}H_x and NaH. By comparison with the hydrogen dehydrogenation peak of NaH itself, the decomposition of the remaining NaH in the mixture could be occurred around 300 °C. Figure 1(b) shows the TG and DSC profiles for the C^{nano}H_x and NaH composite. The DSC spectrum indicates that both the reactions at the sub and the main peaks in the TDMS spectrum at 260 and 300 °C are endothermic, suggesting that the reactions are rechargeable. Additionally, the weight loss of the composite was estimated to be ~5 mass% as shown in the TG profile, though the weight loss due to the decomposition of

lone NaH in the composite is theoretically estimated to ~2 mass%. This suggests that the hydrogen desorption peaked around 260°C is originated in both of NaH and the $C^{\text{nano}}H_x$ products due to the interaction between these components.

Figure 1(c) shows the XRD profile for the $C^{\text{nano}}H_x$ and NaH composite before and after the thermal gas-desorption examination. Mainly, the peaks corresponding to the NaH phase are observed in the XRD profile for the as-milled composite because the $C^{\text{nano}}H_x$ phase itself does not show any diffraction peaks [17]. The XRD profile of the composite after increasing temperature up to 350 °C indicates only the appearance of metallic Na phase. This fact shows that the hydrogen desorption is at least caused by the decomposition of NaH. Moreover, since hydrogen in the $C^{\text{nano}}H_x$ phase is also destabilized by making composite with NaH, a composite of C^{nano} and Na could be supposed to be formed after the dehydrogenation on the analogy of the Li-C-H system [23]. However, the metallic Na phase is clearly observed in the XRD profile, indicating that not only the nano-composite phase between C^{nano} and Na but also the separated phases of C^{nano} and Na are also formed after the dehydrogenation. This behavior seems to be originated in a quite low melting point of Na (below 100 °C).

3.2 Hydrogen storage properties of the $C^{\text{nano}}H_x$ +MgH₂ composite

The $C^{\text{nano}}H_x$ and MgH₂ composite desorbs hydrogen with two peaks as shown in Figure 2(a). The first and second hydrogen desorption peaks were located around 300 and 450 °C, respectively. The first hydrogen desorption temperature was lower than ~350 °C, which seems to correspond to the typical decomposition temperature of pure MgH₂ milled for 2 h [24, 25]. Actually, the metallic Mg phase appears in the XRD profile after desorbing hydrogen at 350 °C as shown in Figure 2(c). Moreover, the TG

profile of the composite as shown in Figure 2(b) reveals ~3 mass% weight loss until 350 °C, where the weight loss is consistent with the calculated value of hydrogen desorption due to decomposition of pure MgH₂ in the composite, indicating that only the decomposition of MgH₂ occurs until 350 °C. Actually, this hydrogen desorption temperature of MgH₂ should be affected by the existence of the C^{nano}H_x product, because the catalytic effect of single wall carbon nano-tubes or graphite powder for the MgH₂ product have already been reported [26-28]. Anyway, the above results suggest that the MgH₂ solid phase does not such strongly interact with the C^{nano}H_x product and the hydrogen in the C^{nano}H_x product is not desorbed at the same temperature as MgH₂ desorbs hydrogen.

On the other hand, when the temperature was increased up to 500 °C corresponding to a higher temperature than a second hydrogen desorption peak one, no evident peak appears in the XRD profile, indicating that a nano-structural cluster composed of a metallic Mg and nano-structural carbon is generated even at 500 °C after desorbing hydrogen by an interaction between Mg and C^{nano}H_x. Actually, the amount of the corresponding hydrocarbons is quite small compared with that from C^{nano}H_x itself in the TDMS spectrum. This result indicates that hydrogen is desorbed instead of hydrocarbon due to destabilization of hydrocarbons group in the C^{nano}H_x product by an interaction with the Mg solid phase. The total amounts of weight loss reach up to ~10 mass% with increasing temperature up to 500 °C in the TG spectrum as shown in Fig. 2 (b). The dehydrogenated C^{nano} and Mg product can potentially be rehydrogenated because two endothermic peaks clearly appear at 300 and 450 °C in the DSC spectrum, respectively.

3.3 Hydrogen storage properties of the C^{nano}H_x+CaH₂ composite

As is shown in Figure 3(a), the hydrogen desorption spectrum for the $C^{\text{nano}}H_x$ and CaH_2 composite shows a two-peak structure in the temperature range from 300 to 500 °C, where the CaH_2 hydride itself could not be decomposed by heating up to 500 °C. Furthermore, a small amount of hydrocarbons desorption drastically decrease from second hydrogen desorption peak at ~450 °C in the TDMS spectrum by making composite of $C^{\text{nano}}H_x$ with CaH_2 , suggesting that hydrocarbons desorption is suppressed compared with that from the $C^{\text{nano}}H_x$ product itself [14]. This indicates that the C-H bonding in the polarized hydrocarbon groups in the $C^{\text{nano}}H_x$ product is weakened by an interaction between CaH_2 and $C^{\text{nano}}H_x$. Then, the composite exhibits a weight loss of ~8 mass% in the TG profile by heating up to 500 °C as shown in Figure 3(b), where the weight loss caused by decomposition of lone CaH_2 is theoretically estimated to ~2 mass% in the composite. This suggests that hydrogen in the $C^{\text{nano}}H_x$ product is desorbed at the same temperature as CaH_2 desorbs hydrogen as well. Thermal analysis due to the DSC measurement indicates that the hydrogen desorption reaction of the composite is weakly endothermic as shown in Fig. 3(b). This result suggests that the rehydrogenation reaction is expected to occur in the $C^{\text{nano}}H_x$ and CaH_2 composite similar to the other metal-C-H materials.

Figure 3(c) shows the XRD profiles for the $C^{\text{nano}}H_x$ and CaH_2 composite. After increasing temperature up to 500 °C, the intensity corresponding to CaH_2 in the XRD profile is significantly suppressed compared with that before the dehydrogenation, where some weak peaks in the XRD profiles indicate that the CaH_2 product was consumed by a reaction between the $C^{\text{nano}}H_x$ and CaH_2 . But the reaction should not be completely finished below 500 °C as shown in Fig 3(a). Furthermore, the XRD profile of the composite exhibits no existence of Ca or CaC_2 after the dehydrogenation at

500 °C. Therefore, it is suggested that a nano-structural cluster composed of C^{nano} and Ca is formed in the composite after the dehydrogenation.

4. CONCLUSION

In this work, the following universal characteristic features on the hydrogen desorption have been found for all the composites of $C^{\text{nano}}H_x$ and MH (M) prepared by a mechanical ball-milling method. The hydrogen desorption temperatures become significantly lower than those of the corresponding hydrides ($C^{\text{nano}}H_x$, MH) by making composite of $C^{\text{nano}}H_x$ with MH. At the same time, significant suppression of hydrocarbons desorption is realized by making composite of $C^{\text{nano}}H_x$ with MH as well, even though $C^{\text{nano}}H_x$ itself releases a considerably large amount of hydrocarbons. This indicates that hydrogen desorption instead of hydrocarbons desorption is induced by a destabilization due to an interaction between the polarized hydrocarbon groups in the $C^{\text{nano}}H_x$ product and MH (or M). Moreover, the ballmilled mixtures composed of the $C^{\text{nano}}H_x$ product and LiH [23], MgH_2 or CaH_2 form a nano-structural cluster composed of nano-structural carbon (C^{nano}) and M after the hydrogen desorption.

Therefore, these thermal gas-desorption and structural properties indicate that an interaction exists between $C^{\text{nano}}H_x$ and MH, and destabilizes some polarized C-H groups in the $C^{\text{nano}}H_x$ product and/or M(-H).

ACKNOWLEDGEMENT

This work was supported by the Grant-in-Aid for COE Research (No. 13CE2002) of the Ministry of Education, Sciences and Culture of Japan and by the project “Development for Safe Utilization and Infrastructure of Hydrogen Industrial

Technology” in NEDO, Japan.

REFERENCES

- [1] A.C. Dillon, K.M. Jones, T.A. Bekkedahl, C.H. Kiang, D.S. Bethune and M.J. Heben, *Nature* 386 (1997) 377.
- [2] Y. Ye, C.C. Ahn, C. Witham, B. Fultz, J. Liu, A.G. Rinzler, D. Colbert, K.A. Smith and R.E. Smalley, *Appl. Phys. Lett.* 74 (1999) 2307.
- [3] P. Chen, X. Wu, J. Lin and K.L. Tan, *Science* 285 (1999) 91.
- [4] C. Liu, Y.Y. Fan, M. Liu, H.T. Cong, H.M. Cheng and M.S. Dresselhaus, *Science* 286 (1999) 1127.
- [5] A.C. Dillon and M.J. Heben, *Applied Physics a-Materials Science & Processing* 72 (2001) 133.
- [6] A. Zuttel, C. Nutzenadel, P. Sudan, P. Mauron, C. Emmenegger, S. Rentsch, L. Schlapbach, A. Weidenkaff and T. Kiyobayashi, *J. Alloys Compd.* 330 (2002) 676.
- [7] H. Kajjura, S. Tsutsui, K. Kadono, M. Kakuta, M. Ata and Y. Murakami, *Appl. Phys. Lett.* 82 (2003) 1105.
- [8] C. Park, P.E. Anderson, A. Chambers, C.D. Tan, R. Hidalgo and N.M. Rodriguez, *J. Phys. Chem. B* 103 (1999) 10572.
- [9] H. Takagi, H. Hatori, Y. Soneda, N. Yoshizawa and Y. Yamada, *Materials Science and Engineering B-Solid State Materials for Advanced Technology* 108 (2004) 143.
- [10] H. Takagi, H. Hatori and Y. Yamada, *Carbon* 43 (2005) 3037.
- [11] K.A.G. Amankwah and J.A. Schwarz, *Carbon* 33 (1995) 1313.
- [12] S. Hynek, W. Fuller and J. Bentley, *Int. J. Hydrogen Energy* 22 (1997) 601.
- [13] S. Orimo, G. Majer, T. Fukunaga, A. Zuttel, L. Schlapbach and H. Fujii, *Appl. Phys. Lett.* 75 (1999) 3093.
- [14] S. Orimo, T. Matsushima, H. Fujii, T. Fukunaga and G. Majer, *J. Appl. Phys.* 90 (2001) 1545.
- [15] D.M. Chen, T. Ichikawa, H. Fujii, N. Ogita, M. Udagawa, Y. Kitano and E. Tanabe, *J. Alloys Compd.* 354 (2003) L5.
- [16] T. Ichikawa, D.M. Chen, S. Isobe, E. Gomibuchi and H. Fujii, *Materials Science and Engineering B-Solid State Materials for Advanced Technology* 108 (2004) 138.
- [17] S. Isobe, T. Ichikawa, J.I. Gottwald, E. Gomibuchi and H. Fujii, *J. Phys. Chem. Solids* 65 (2004) 535.
- [18] M. Hirscher and B. Panella, *J. Alloys Compd.* 404 (2005) 399.
- [19] N. Ogita, K. Yamamoto, C. Hayashi, T. Matsushima, S. Orimo, T. Ichikawa, H. Fujii and M. Udagawa, *J. Phys. Soc. Jpn.* 73 (2004) 553.
- [20] T. Fukunaga, K. Itoh, S. Orimo and K. Aoki, *Materials Science and Engineering B-Solid State Materials for Advanced Technology* 108 (2004) 105.
- [21] T. Ichikawa, S. Isobe and H. Fujii, *Materials Transactions* 46 (2005) 1757.
- [22] T. Ichikawa, N. Hanada, S. Isobe, H.Y. Leng and H. Fujii, *Journal of Physical Chemistry B* 108 (2004) 7887.

- [23] T. Ichikawa, H. Fujii, S. Isobe and K. Nabeta, *Appl. Phys. Lett.* 86 (2005)
- [24] N. Hanada, T. Ichikawa and H. Fujii, *Journal of Physical Chemistry B* 109 (2005) 7188.
- [25] N. Hanada, I. Ichikawa and H. Fujii, *J. Alloys Compd.* 404 (2005) 716.
- [26] H. Imamura, S. Tabata, N. Shigetomi, Y. Takesue and Y. Sakata, *J. Alloys Compd.* 330 (2002) 579.
- [27] C.X. Shang and Z.X. Guo, *J. Power Sources* 129 (2004) 73.
- [28] C.Z. Wu, P. Wang, X.D. Yao, C. Liu, D.M. Chen, G.Q. Lu and H.M. Cheng, *Journal of Physical Chemistry B* 109 (2005) 22217.

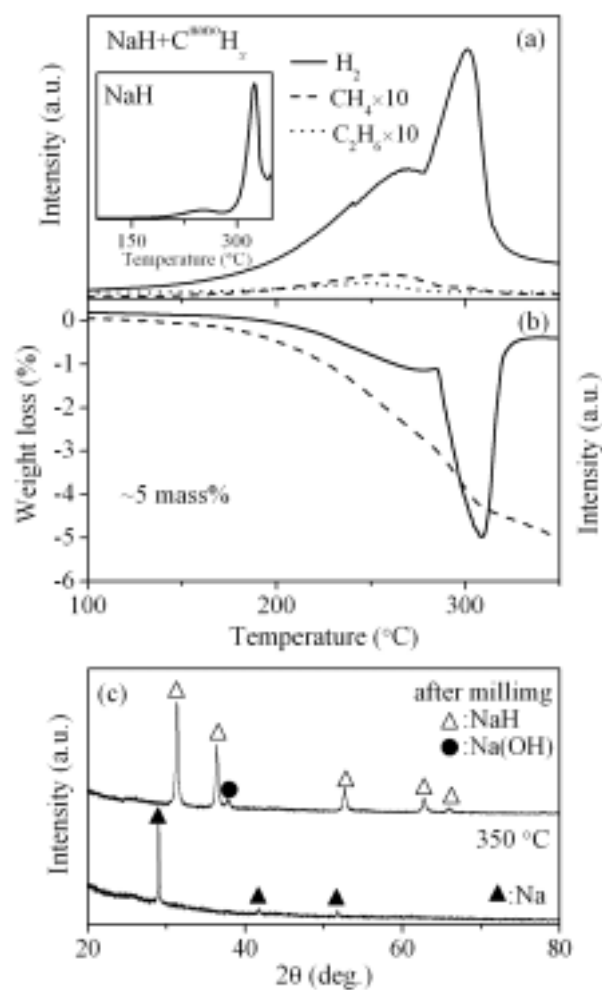


Figure 1. (a) Thermal desorption mass spectroscopy (TDMS) profiles of hydrogen and hydrocarbons from the $\text{C}^{\text{nano}}\text{H}_x$ and NaH composite, where the intensity of hydrocarbons is enlarged ten times, and the inset shows TDMS profile of the milled NaH ; (b) weight loss (TG: dashed line) and differential scanning calorimetry (DSC: solid line) spectra for the $\text{C}^{\text{nano}}\text{H}_x$ and NaH composite; (c) the XRD profiles after milling and after heating up to $350 \text{ }^{\circ}\text{C}$ for the thermal analysis for the $\text{C}^{\text{nano}}\text{H}_x$ and NaH composite.

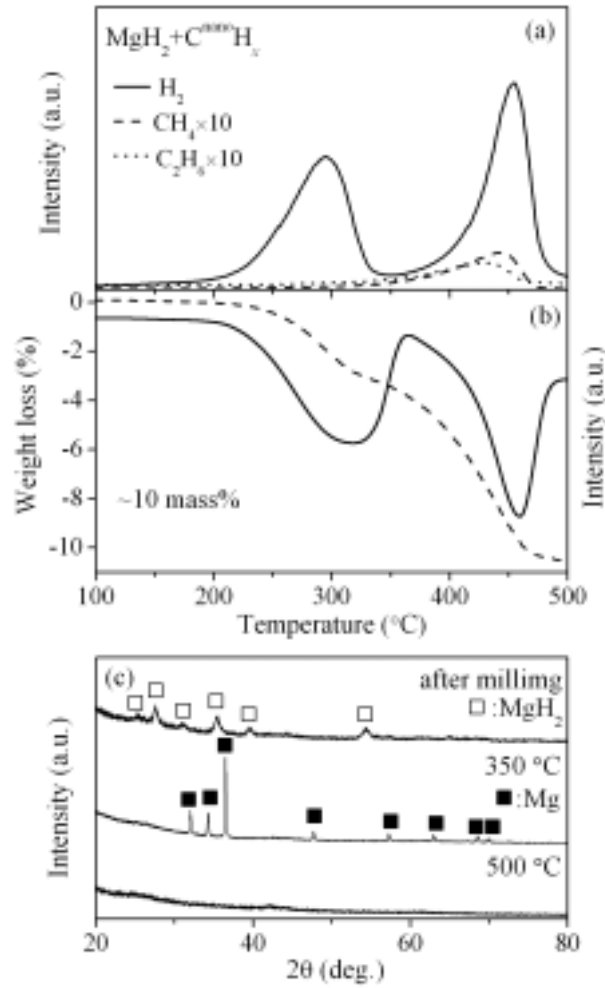


Figure 2. (a) Thermal desorption mass spectroscopy (TDMS) profiles of hydrogen and hydrocarbons from the $\text{C}^{\text{nano}}\text{H}_x$ and MgH_2 composite, where the intensity of hydrocarbons are enlarged ten times; (b) weight loss (TG: dashed line) and differential scanning calorimetry (DSC: solid line) spectra for the $\text{C}^{\text{nano}}\text{H}_x$ and MgH_2 composite; (c) the XRD profiles after milling, after heating up to 350 $^{\circ}\text{C}$ and 500 $^{\circ}\text{C}$ for the thermal analysis of the $\text{C}^{\text{nano}}\text{H}_x$ and MgH_2 composite.

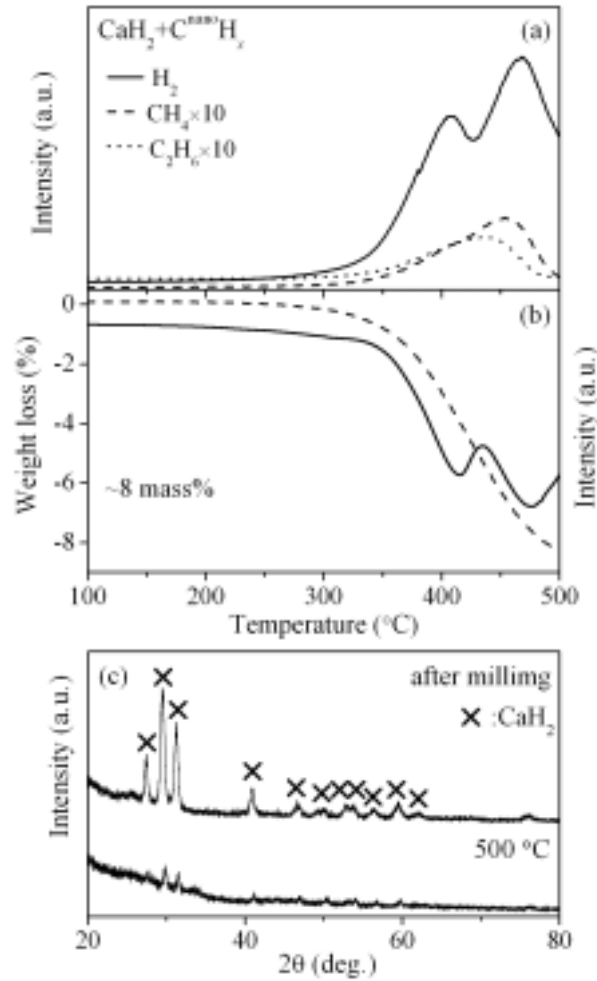


Figure 3. (a) Thermal desorption mass spectroscopy (TDMS) profiles of hydrogen and hydrocarbons from the $\text{C}^{\text{nano}}\text{H}_x$ and CaH_2 composite, where the intensity of hydrocarbons are enlarged ten times; (b) weight loss (TG: dashed line) and differential scanning calorimetry (DSC: solid line) spectra for the $\text{C}^{\text{nano}}\text{H}_x$ and CaH_2 composite; (c) the XRD profiles after milling, after heating up to 500 $^{\circ}\text{C}$ for the thermal analysis of the $\text{C}^{\text{nano}}\text{H}_x$ and CaH_2 composite.